

# Dimethyl fumarate attenuates MSU-induced gouty arthritis by inhibiting NLRP3 inflammasome activation and oxidative stress

Y. CAO, Y. HU, X.-F. JIN, Y. LIU, J.-M. ZOU

Department of Rheumatology, The First People's Hospital of LouDi, LouDi, Hunan, China

**Abstract. – OBJECTIVE:** Dimethyl fumarate (DMF) has shown anti-inflammatory and antioxidant activities. However, the effects of DMF on gouty arthritis remain elusive, and the underlying mechanism is not understood. In this study, we aim to investigate the role of DMF in gouty arthritis.

**MATERIALS AND METHODS:** Mice were gavage with DMF for consecutive 7 days at two different doses (10 mg/kg/day or 30 mg/kg/day, once daily) in advance and then monosodium sodium urate (MSU) was injected into their joint to establish an acute gout mice model. The pain and swelling of the hind paw in mice were determined. The production of pro-inflammatory cytokine in the paw tissues was assessed by Elisa and the inflammatory infiltration of the joint was determined by hematoxylin and eosin (H&E) staining. The activity of superoxide dismutase (SOD) and the content of malondialdehyde (MDA) in the tissues were measured by commercial kits. In addition, the expression of nuclear factor kappa B (NF- $\kappa$ B) and NACHT, LRR, and PYD domains-containing protein 3 (NLRP3) inflammasome and downstream genes were detected by PCR and Western blot. Furthermore, LPS-primed murine macrophages Raw 264.7 cells were treated with different concentrations of DMF (2  $\mu$ M, 5  $\mu$ M, 10  $\mu$ M) for 2 h, and then challenged with MSU (200  $\mu$ g/mL) for other 12 h to observe the effect of DMF on cell viability via cell counting kit-8 (CCK-8) assay and lactate dehydrogenase (LDH) levels in the supernatant of culture medium. Immunofluorescent staining was used to detect the NLRP3 inflammasome activation and reactive oxygen species (ROS) production in vitro. Caspase-1 activity was measured by corresponding assay kits both in vivo and in vitro.

**RESULTS:** DMF attenuated pain and swelling in MSU-induced gout mice by decreasing pro-inflammatory cytokine production and inflammatory cell infiltration, as well as improved oxidative stress. Moreover, DMF inhibited the activation of NF- $\kappa$ B and NLRP3 inflammasome and subsequent expression of caspase-1, interleukin-1 $\beta$  (IL-1 $\beta$ ), and IL-18 at both mRNA and pro-

tein levels. Meanwhile, DMF suppressed NLRP3 inflammasome expression and ROS production in LPS and MSU-stimulated Raw 264.7 cells, thereby protecting the cells from inflammatory injury.

**CONCLUSIONS:** DMF serves as a new approach for the treatment of MSU-induced gouty arthritis by suppressing NLRP3 inflammasome activation and oxidative stress.

*Key Words:*

Dimethyl fumarate, Gouty arthritis, NLRP3 inflammasome, Oxidative stress.

## Introduction

Gouty arthritis is a common inflammatory disease, mainly due to hyperuricemia caused by monosodium sodium urate (MSU) crystal deposition in the capsule, bursa, cartilage, bone, and other tissues, resulting in acute joint inflammation<sup>1</sup>. Current anti-inflammatory corticosteroids are limited by potential drug toxicities, and gaps in therapeutic efficacy are far from satisfactory<sup>2</sup>. Moreover, only 50% of gouty arthritis patients are responsive to current clinical agents<sup>3,4</sup>. Therefore, an unmet clinical is needed to exploit a new target and more efficient and safer drug for treating gouty arthritis.

As a member of nucleotide-binding oligomerization domain-like (NOD-like) receptors in the innate immune system, the NACHT, LRR, and PYD domains-containing protein 3 (NLRP3) inflammasome are associated with the MSU crystal-driven gouty arthritis due to excessive inflammatory response<sup>5,6</sup>. The NLRP3 inflammasome is a cytosolic multiprotein assembly consisting of NLRP3, apoptosis-associated speck-like protein (ASC), and precursor caspase-1 (pro-caspase1)<sup>7</sup>. MSU crystals recruit nucleotide-binding oligomerization NLRP3 to the release of inflamma-

tory mediators, such as interleukin-1 $\beta$  (IL-1 $\beta$ ) and IL-18, accompanied by increasing levels of cytokines interleukin-6 (IL-6) and tumor necrosis factor  $\alpha$  (TNF- $\alpha$ )<sup>8,9</sup>. In the early stage, macrophages sense MSU crystals in an NLRP3 inflammasome-dependent manner, and then initiate the expression of functional inflammasome components, such as NLRP3, pro-IL-1 $\beta$ , and pro-IL-18 *via* the nuclear factor kappa B (NF- $\kappa$ B) signaling pathway<sup>10,11</sup>. Next, the formation of ASC oligomers, ASC specks, as well as caspase-1 promoted by the damage-associated molecular patterns (DAMPs), cleaves pro-IL-1 $\beta$  and pro-IL-18 into their biologically active form IL-1 $\beta$  and IL-18, which worsen the inflammatory response during the MSU induced gout<sup>11,12</sup>. Moreover, previous studies<sup>13,14</sup> have reported that redox signaling molecules such as reactive oxygen species (ROS) also mediate the formation of the NLRP3 inflammasome, thus interfering with acute gouty arthritis. Further investigations are required to develop a comprehensive understanding of these dynamic processes and better therapeutic strategies for gouty arthritis associated with NLRP3 inflammasome.

Dimethyl Fumarate (DMF) is a Food and Drug Administration (FDA) approved drug for Relapsing-Remitting Multiple Sclerosis (RRMS) since early 2010<sup>15,16</sup>. *In vivo* and *in vitro* studies<sup>17,18</sup> have proven that DMF possesses immunomodulatory, anti-inflammatory, anti-oxidative, and neuroprotective properties. The protective nature of DMF has been attributed to inhibiting the pro-inflammatory pathway NF- $\kappa$ B, thus downregulating the expression of NLRP3 and suppressing inflammatory response in multiple inflammatory disease models<sup>18,19</sup>. However, DMF's effects and the intrinsic mechanism on NLRP3 inflammasome in gouty arthritis remain unexplored, since there was currently no relevant experimental study available.

In the present study, we investigated the effect of DMF on gouty arthritis model in mice by detecting paw swelling, pain, and inflammatory response. We hypothesized that DMF would exert protective effects against the NLRP3 inflammasome activation and production of ROS in MSU-stimulated mice. Later, the beneficial effect of DMF was also verified in the MSU-treated Raw 264.7 cells. Taken together, this study suggested that DMF inhibited NLRP3 inflammasome activation and oxidative stress, thereby alleviating NLRP3-dependent gouty arthritis, which affirms DMF as a potential candidate drug in gouty arthritis treatment.

## Materials and Methods

### Animals

Male 7-8 weeks C57BL/6 mice (23  $\pm$  2 g) were purchased from Gempharmatech Co., Ltd (Nanjing, Jiangsu, China). The mice were housed six per cage under specific pathogen-free (SPF) conditions (12 h light/dark cycles and 24  $\pm$  2°C) for 7 days to adapt to the new environment before starting experiments. Food and water were freely available to the animals. Animal welfare and experimental procedures were carried out strictly by the Guide for the Care and Use of Laboratory Animals (National Institutes of Health).

### Reagents

Dimethyl fumarate (#PHR2118), Uric Acid Sodium Salt (#U2875), and Lipopolysaccharides (LPS) were purchased from Sigma-Aldrich (St Louis, MO, USA). Mouse IL-1 $\beta$ , IL-6, IL-18, and TNF- $\alpha$  ELISA kits were purchased from Nanjing Jiancheng Bioengineering Institute (Nanjing, Jiangsu, China). MDA and SOD assay kits were purchased from Beyotime Biotechnology (Shanghai, China). Primary antibodies against NLRP3 (#PA5-79740) and caspase-1 (#PA5-87536) were purchased from Invitrogen Inc. (Thermo Fisher Scientific, Waltham, Massachusetts, USA), NF- $\kappa$ B (#ab76302), IL-18 (#ab243091) and IL-1 $\beta$  (#ab254360) and secondary antibody (#ab6789) were purchased from Abcam Inc (Boston, MA, USA).

### Mice Model of Acute Gouty Arthritis and Experimental Design

The mice were randomly divided into the following group (n = 6 per group): Control group, MSU group, MSU+10 mg/kg DMF and MSU+30 mg/kg DMF. The treatment of DMF (10 mg/kg or 30 mg/kg, dissolved in saline, I.P) was performed once daily for consecutive 7 days<sup>17,20</sup>. Gouty arthritis is initiated by the deposition of MSU crystal around the joints. Therefore, the acute gouty arthritis model was established by injection of MSU crystal into the ankle joint of rodents as previously described<sup>21</sup>. On the seventh day, 3 mg of MSU crystals resuspended in 70  $\mu$ L of sterile Phosphate-Buffered Saline (PBS) were injected *via* the subcutaneous route into the left hind paws of mice 1 h after DMF administration. Mice in the Control group received injection of 70  $\mu$ L sterile PBS. The experiment samples *in vivo* were from these groups. The doses of DMF and MSU were chosen based on the literature and our preliminary experiments<sup>17,20,21</sup>.

### **Assessment of Gouty Arthritis: Ankle Joint Edema Evaluation, Mechanical Hyperalgesia, and Thermal Sensitivity Determination**

The circumference of ankle is a visual indicator of the degree of swelling in the joint<sup>9</sup>. Ankle joint swelling was measured with an electronic caliper at the same indicated time points (4, 8, 12, 24 h). The circumference of these time points and the increment of the circumference between adjacent points were analyzed.

Measuring inflammation-induced changes in thresholds of hind paw withdrawal from mechanical pressure is a useful technique to assess mechanical hyperalgesia in gouty arthritis mice model<sup>22</sup>. An electronic von Frey apparatus from Wanger Instruments (Greenwich, CT, USA) allows precise assessment of mouse hind paw withdrawal thresholds. In brief, the mice were acclimated to individual chambers placed on a wire mesh floor with full contact of the hind paw with Von Frey filaments. Mice were habituated for 15 min before the test, and then withdrawal threshold were measured two times using each Von Frey filaments for 6-8 s to achieve maximum mechanical stimulation. Each 50% paw withdrawal threshold was obtained, and average value was used for statistical analysis.

As previously described, the thermal sensitivity of mice was determined using a thermal testing apparatus from Ugo Basile (Gemonio, VA, Italy)<sup>23</sup>. Briefly, mice were placed on the platform of thermal testing apparatus and adapted to warmed glass surface for 15 min. The paw withdrawal latency was recorded from the onset of the irradiation (lamp 40 W, distance lamp to paw 40 mm) to the withdrawal of the hind paw at 25°C. The paw withdrawal latency time were measured three times with a minimum interval of 5 min, and average latency time was used for statistical analysis.

### **Cytokine Analysis by Elisa**

Hind paw tissue was collected, and the production of cytokine was measured by ELISA assay kits for IL-1 $\beta$ , IL-6, IL-18 and TNF- $\alpha$  according to the manufacturer's instructions.

### **H&E Staining**

Hind paw tissue was dissected 24 h after MSU crystal injection, fixed with 10% paraformaldehyde in PBS, and then paraffin embedded sections were deparaffinized, rehydrated, and washed in water. The paraffin sections were stained with hematoxylin and eosin (H&E) for conventional

morphological evaluation using a light microscope on 20 $\times$  objective.

### **Evaluation of Oxidative Stress Status in Vivo: the Activity of SOD and the Content of MDA**

As indicators of oxidative stress, the superoxide dismutase (SOD) activity and the malondialdehyde (MDA) levels in the hind paw tissue were detected by using the commercially assay kits from Beyotime Biotechnology (Shanghai, China) according to the manufacturer's instructions.

### **Real-Time PCR**

RNA was extracted from the paw tissue using the TRIzol method. cDNA was synthesized from RNA using FastKing One Step RT-PCR Kit from Tiangen Biotech Co., LTD (Beijing, China). All primers were purchased from the TSINGKE Biosystems (Beijing, China). Quantitative real-time PCR was performed with SYBR Green from Bio-Rad (Hercules, CA, USA). Gene expression was calculated by the  $2^{-\Delta\Delta C_t}$  method and normalized to the GAPDH levels. The sequences of all primers used were as follows:

GAPDH: F,5'-ATCTTTTGGGGTCCGTC AACT-3';  
R,5'-TTTGC ACTGGTACGTGTTGAT-3';  
IL-1 $\beta$ : F,5'-CAACTGTTCTGA ACTCAACTG-3';  
R,5'-GAAGGAAAAGAAGGTGCTCATG-3';  
caspase-1: F,5'-AGAGGATTTCTTAACGGATG-  
CA-3'; R,5'-TCACAAGACCAGGCATATTCTT3';  
NLRP3: F,5'-ATGTGAGAAGCAGGTTCTACTC-3';  
R,5'-CTCCAGCTTAA GGGA ACTCATG-3';  
IL-18: F,5'-TGATGAGCTGGAATGCGATGCC-3';  
R,5'-TGGACGAACCACAAGCAACTGG-3'.

### **Caspase-1 Activity Assay**

Caspase-1 activity was measured by the caspase-1 activity assay kit from Abcam Inc (Boston, MA, USA) according to the manufacturer's recommendations. This assay kit is based on the ability of caspase-1 to catalyze the specific substrate N-acetyl-Tyr-Val-Ala-Asp p-nitroanilide (Ac-YVAD pNA) to release free p-nitroaniline (pNA), which has strong absorption at 405 nm, and then the activity of caspase-1 in cells was analyzed by detecting the absorbance of pNA using a standard pNA curve. Caspase-1 activity was calculated as the percentage of untreated cells.

### **Western Blotting Analysis**

Protein from the ankle joint and surrounding tissue was extracted by the RIPA lysis buffer from Beyotime Biotechnology (Shanghai, China) sup-

plemented with PMSF from Roche (Basel, Switzerland) and protease inhibitor cocktail from Beyotime Biotechnology and then adjusted to the same concentration. 30 µg protein was loaded and separated by sodium dodecyl sulfate-polyacrylamide gel electrophoresis (SDS-PAGE) and then transferred to the polyvinylidene fluoride (PVDF) membranes. After blocking with 5% bovine serum albumin (BSA) for 1 h at room temperature, the membranes were incubated with the primary antibodies at 4°C overnight (NF-κB: 1:1,000, NLRP3: 1:1,000, caspase-1: 1:1,000, IL18: 1:1,000, IL-1β: 1:1,000). On the second day, the membrane was incubated with an HRP-conjugated antibody (1:10,000) at room temperature for 1 h. Protein bands were exposed with enhanced chemiluminescence solution. The gray value of the strips was analyzed by ImageJ software.

### **Cell Culture and Drug Treatment**

Raw 264.7 murine macrophage cells were purchased from Cell Bank of the Chinese Academy of Sciences (Shanghai, China) and cultured in Dulbecco's Modified Eagle's medium (DMEM, High Glucose) complete medium supplemented with 10% (v/v) fetal bovine serum (FBS; Biological Industries), 100 U/mL penicillin, and 100 mg/mL streptomycin under a humidified 5% (v/v) CO<sub>2</sub> atmosphere at 37°C. The third generation of Raw 264.7 cells were used to incubate in 6-well plate and randomly divided into control group, MSU group, MSU+DMF group. Cells of MSU +DMF group were stimulated with 100 ng/ml LPS for 2 h, followed by different concentrations of DMF (2 µM, 5 µM, 10 µM) for 2 h, and then treated with MSU (200 µg/mL) for another 12 h according to the previous literature<sup>24,25</sup>. All treatments conditions in MSU group were the same as those in MSU+DMF group, except the addition of DMF.

### **LDH Assay**

LDH is the most widely used marker to run a cytotoxicity assay. LDH assay kit from Abcam Inc (Boston, MA, USA) was used to determine the LDH release in the supernatant of cell culture medium by following the manufacturer's protocol. The colorimetric change of cells at 492 nm was obtained with a microplate reader Varioskan from Thermo Fisher (Waltham, MA, USA). The LDH (U/ml) of the sample was calculated according to the LDH standard curve.

### **Immunofluorescent Staining**

Briefly, the treated cells were cultured in confocal dishes, and then were incubated with primary

antibodies NLRP3 and caspase-1. After 3-times washing with PBS, cells were incubated with the appropriate secondary antibodies. DAPI Staining Solution (#C1005) from Beyotime Biotechnology (Shanghai, China) was applied as a marker for cell nuclei. Images were captured by using a fluorescence microscopy from Olympus (Tokyo, Japan).

### **Cell Viability Assay**

5×10<sup>3</sup> Cells per well were cultured in a 96-well plate. After 12 h, cells were stimulated with different concentrations of DMF for 2 h and then incubated with 10 µL cell counting kit-8 (CCK-8) from Sigma-Aldrich, Inc. (St. Louis, MO, USA) reagent for 2 h. Colorimetric change of cells was measured at 450 nm as an indicator of cell activity. Cell viability percentages were calculated as the percentage of untreated cells.

### **Detection of Oxidative Stress In Vitro**

Intracellular reactive oxygen species (ROS) level was detected by the membrane-permeable ROS-sensitive fluorescent indicator, 2',7'-dichlorodihydro-fluorescein diacetate (DCFH-DA) using the ROS Assay Kit from Beyotime Biotechnology (Shanghai, China) according to the manufacturer's instruction. The level of intracellular ROS was recorded by fluorescence microscopy and calculated by ImageJ software.

### **Statistical Analysis**

GraphPad Prism v.8.4.3 (La Jolla, CA, USA) was employed for statistical analysis. The Shapiro-Wilk normality test was performed to determine the data distribution. Data were normally distributed and presented as the mean ± standard deviation (SD). One-way analysis of variance (ANOVA), followed by Tukey's multiple comparisons test, was performed to determine the differences among > 2 groups. *p*-values < 0.05 were considered significant.

## **Results**

### **DMF Alleviated Gouty Arthritis Related Symptoms in C57/BL6 Mice Induced by MSU**

To determine whether there would be beneficial effect of DMF on acute gouty arthritis, we first administered DMF at two different doses (10 mg/kg/day or 30 mg/kg/day, I.P) for seven days. Subsequently, a mice model of acute gouty arthritis was established by injection of MSU into the left



hind paw (Figure 1A). The swelling, mechanical hypersensitivity, and thermal sensitivity of paw were measured at several key points after model establishment (4, 8, 12, 24 h). Compared with the control mice, injected with PBS alternatively, MSU-induced ones exhibited typical acute symptoms, including severe paw swelling, mechanical hyperalgesia, and thermal sensitivity (Figure 1B-I). The results suggested that treatment with DMF (both 10 mg/kg/day and 30 mg/kg/day) relieved these symptoms or index triggered by MSU. Interestingly, the improvement was more pronounced in the group treated with 30 mg/kg DMF than that of 10mg/kg, which urged us to apply the group of 30 mg/kg DMF in the following experiments to investigate the underlying mechanism. Overall, these results suggested that DMF suppressed the MSU-induced gouty arthritis related symptoms in mice in a dose-dependent manner.

#### ***DMF Reduced the Inflammatory Cytokine Levels, Oxidative Stress, and Inflammatory Cell Infiltration in Gouty Arthritis Mice***

Activation of the inflammatory response induced by sodium urate contributes to the gout arthritis, and we applied DMF at a dose of 30 mg/kg in subsequent experiments to elucidate the underlying mechanisms. Firstly, we detected the level of several crucial inflammatory factors in the collected tissues 24 h after MSU injection. Elisa results showed that MSU-induced inflammatory cytokine (IL-1 $\beta$ , IL-6, IL-18, and TNF- $\alpha$ ) release in the paw tissues was significantly reduced by DMF (Figure 2A-D). Considering the interaction between inflammasome activation and tissue oxidative stress, we detected the degree of oxidative stress in paw tissues reflected by the level of MDA and the activity of antioxidant enzyme SOD. The results suggested that MSU worsen the oxidative stress indicated by increased level of MDA and suppressed SOD activity, whereas DMF alleviated this trend by partially inhibiting the rise of MDA level and promoting the SOD activity (Figure 2E-F). Furthermore, H&E staining also showed that the cells in the paw tissue of the control group were normal without infiltration (Figure 2G). However, tissues of MSU-injected mice appeared to have a severe inflammatory cell infiltration, and the surrounding cells showed a vesicular-like morphology (Figure 2G). As expected, the administration with DMF significantly reversed the inflammatory pathological changes of the paw in gouty arthritis mice (Figure 2G).

Taken together, these results demonstrated that DMF could inhibit inflammatory response and oxidative stress in gouty arthritis.

#### ***DMF Inhibited MSU-Induced NF $\kappa$ B and NLRP3 Inflammasome Activation in Vivo***

MSU-induced production of pro-inflammatory cytokine and those inflammatory symptoms mentioned above is closely associated with NLRP3 inflammasome activation. We next pay attention to the influence of DMF on NLRP3 inflammasome activation after MSU challenge. As is shown in Figure 3A-E, the mRNA expression in paw tissues of NF- $\kappa$ B and related inflammatory genes NLRP3, and downstream genes of caspase-1, IL-1 $\beta$  and IL-18 were markedly enhanced as a result of MSU stimulation. Nonetheless, these genes expression was significantly suppressed by DMF treatment. Similarly, western blot analysis from the tissue sample suggested that MSU promoted the expression of those genes mentioned above, whereas DMF obviously decreased the overexpression of NLRP3, caspase-1, IL-1 $\beta$  and IL-18 at protein level in tissues of gouty arthritis mice (Figure 3F-K). In addition, it is well known that activated NLRP3 recruit caspase-1 to promote pro-inflammatory cytokine maturation. The detection of caspase-1 activity also confirmed that DMF could inhibit the activated caspase-1 caused by NLRP3 inflammasome activation in MSU-induced mice (Figure 3L). Overall, these results demonstrated that DMF inhibited NF- $\kappa$ B and NLRP3 inflammasome activation in MSU-induced gouty arthritis mice.

#### ***DMF Suppressed the Activation of NLRP3 Inflammasome and ROS Production in MSU-Induced Raw 264.7 Cells***

Further investigation of the effects of DMF on NLRP3 inflammasome activation is needed to be verified *in vitro*. Raw 264.7 cells were primed with LPS (100 ng/mL) for 2 h with or without DMF pretreatment for 2 h at various concentrations (2, 5, 10  $\mu$ M) and then stimulated with MSU crystals (200  $\mu$ g/mL) for another 12 h. In the cell CCK-8 assay, we observed a significant decrease in cell viability with LPS and MSU treatment compared to the Raw 264.7 cells without any treatment (Figure 4A). Not surprisingly, DMF treatment raised the cell viability to some extent and this beneficial effect strengthened with the increased concentration of DMF, reaching the peak at 10  $\mu$ M, which has been shown to be effective and safe in previous literature (Figure 4A). Additionally, we

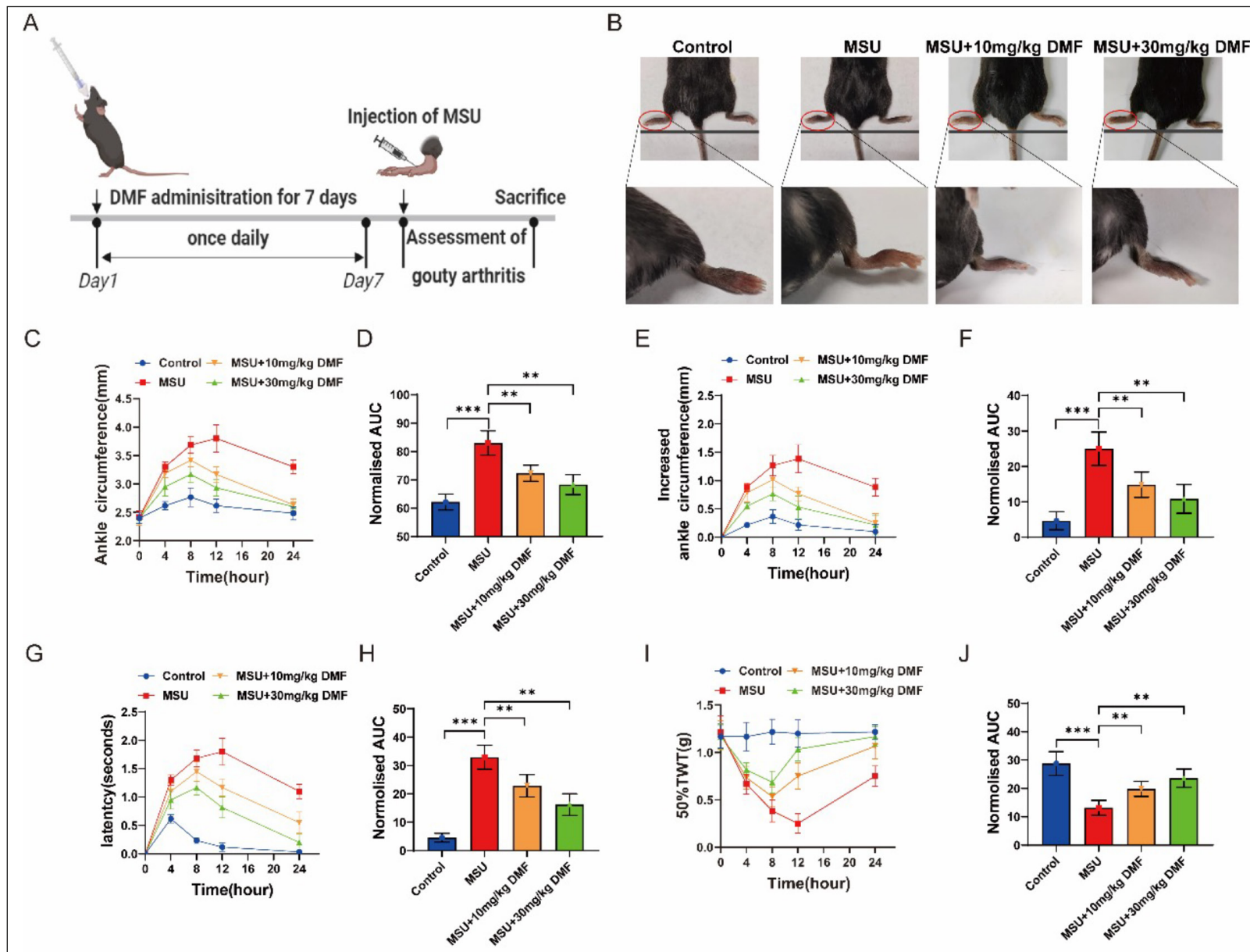


**Figure 1.** DMF alleviated MSU-induced gouty arthritis in C57/BL6 mice. **A**, Experimental scheme of the gouty arthritis model and the administration of DMF. **B**, Representative pictures of foot paw of mice after MSU injection for 24 h. **C**, Paw edema measured at different times after MSU injection. **D**, Normalized AUC (area under curve) of panel (B). **E**, Increased paw thickness measured at different times after MSU injection. **F**, Normalized AUC of panel (E). **G**, The results of thermal sensitivity measured at different times after MSU injection. **H**, Normalized AUC of panel (G). **I**, The results of mechanical allodynia measured at different times after MSU injection. **J**, Normalized AUC of panel (I). The data are expressed as mean  $\pm$  SD of 6 mice in each group. \* $p < 0.05$ , \*\* $p < 0.01$ , and \*\*\* $p < 0.001$ . One-way ANOVA was used for single-factor sample comparisons.

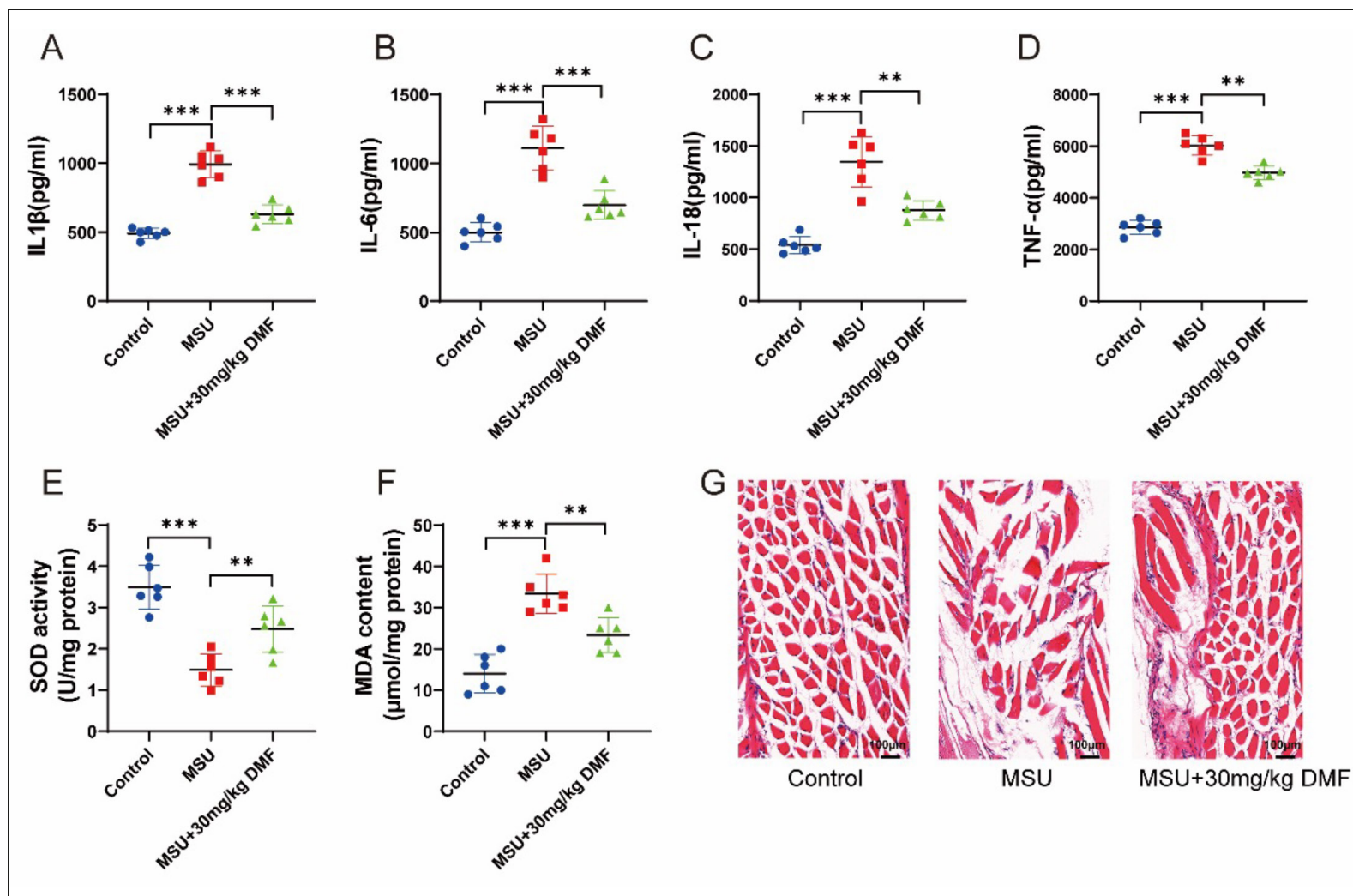


**Figure 2.** DMF attenuated inflammation and oxidative stress in gouty arthritis mice. Elisa results of pro-inflammatory cytokines in the paw tissues of mice in different groups 24 h after model establishment: IL-1 $\beta$  (A), IL-6 (B), IL-18 (C), TNF- $\alpha$  (D). E, SOD activity and (F) MDA level in the paw tissues of mice in different groups 24 h after model establishment. G, H&E staining of the hind paw from different groups. Scale bars: 100  $\mu$ m. The data are expressed as mean  $\pm$  SD of 6 mice in each group. \* $p$  < 0.05, \*\* $p$  < 0.01, and \*\*\* $p$  < 0.001. One-way ANOVA was used for single-factor sample comparisons.

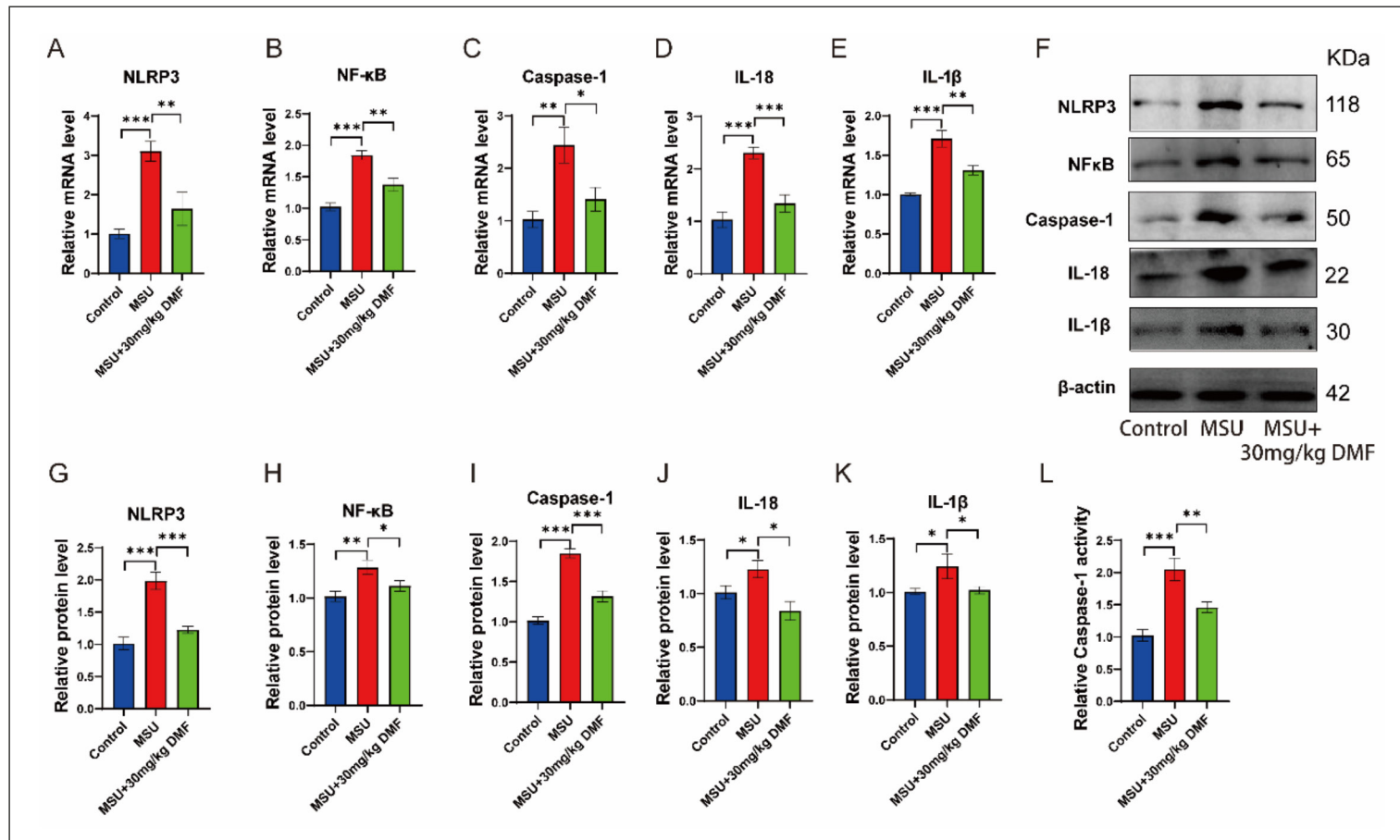


**Figure 3.** DMF suppressed the activation of NF-κB and NLRP3 inflammasome in paw tissue of gouty arthritis mice. **A-E**, The relative mRNA expression of NLRP3 (**A**), NF-κB (**B**), caspase-1 (**C**), IL-1β (**D**), and IL-18 (**E**) in the paw tissues of different group mice. GAPDH was used as the loading control. **F**, Representative western bands of paw tissues from different groups shown in panel. **G-K**, The protein expression of NLRP3 (**G**), NF-κB (**H**), caspase-1 (**I**), IL-1β (**J**), and IL-18 (**K**) in the paw tissues of different group mice. β-actin was used as the loading control. **L**, Relative activity of caspase-1 in tissues from different groups. The data are expressed as mean ± SD of 6 mice in each group. \**p* < 0.05, \*\**p* < 0.01, and \*\*\**p* < 0.001. One-way ANOVA was used for single-factor sample comparisons.



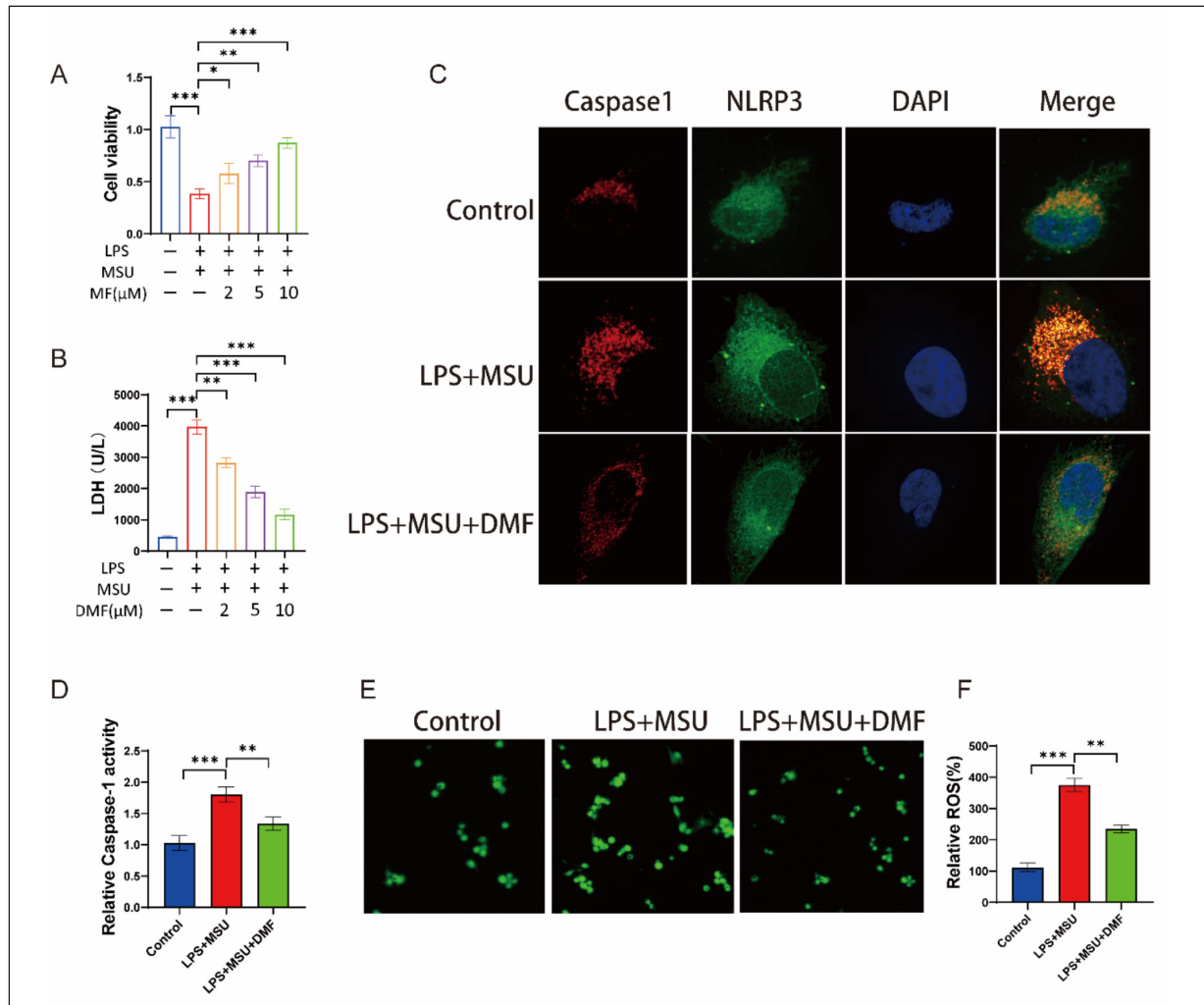


**Figure 4.** DMF inhibited the NLRP3 inflammasome activation and ROS production in response to MSU in LPS-primed Raw 264.7 cells **A**, The results of CCK-8 assay in the LPS and MSU treated Raw 264.7 cells with or without different concentration of DMF. **B**, The LDH level in the supernatant of cell culture medium in the LPS and MSU treated Raw 264.7 cells with or without different concentration of DMF. **C**, Representative groups were stained for caspase-1 (Red) and NLRP3 (Green). DAPI for nuclear staining (Blue). The images were captured under a fluorescence microscope after immunofluorescence staining. Scale bars, 10 μm. **D**, Relative activity of caspase-1 in Raw 264.7 cells after the indicated treatments. **E**, Representative images of DCFH-DA staining in Raw 264.7 cells after the indicated treatments. Scale bars, 50 μm. **F**, The calculated fluorescence intensity of Raw 264.7 cells after the indicated treatments. The data are expressed as mean ± SD of 6 mice in each group. \* $p < 0.05$ , \*\* $p < 0.01$ , and \*\*\* $p < 0.001$ . One-way ANOVA was used for single-factor sample comparisons.

revealed significant protection in cell death with DMF treatment, indicated by the inhibited LDH level in the supernatant of cell culture medium compared to the LPS and MSU treated cells (Figure 4B). We proceeded to detect the expression of NLRP3 and related inflammatory markers caspase-1 by immunofluorescence staining and found that DMF (10 μM) treatment markedly suppressed the expression of NLRP3 and caspase-1 (Figure 4C). Moreover, the caspase-1 activity assay showed that DMF (10 μM) downregulated the caspase-1 activ-

ity in LPS and MSU treated Raw 264.7 cells (Figure 4D). As mentioned above, we finally detected the effect of DMF on the intracellular ROS level by dichloro-dihydro-fluorescein diacetate (DCFH-DA) probe and found that DMF could eliminate the excess production of ROS in LPS and MSU stimulated Raw 264.7 cells, which is consistent with the data *in vivo* (Figure 4E-F). These results supported that DMF exerted protective effects by inhibiting NLRP3 inflammasome activation and ROS generation induced by MSU *in vitro*.

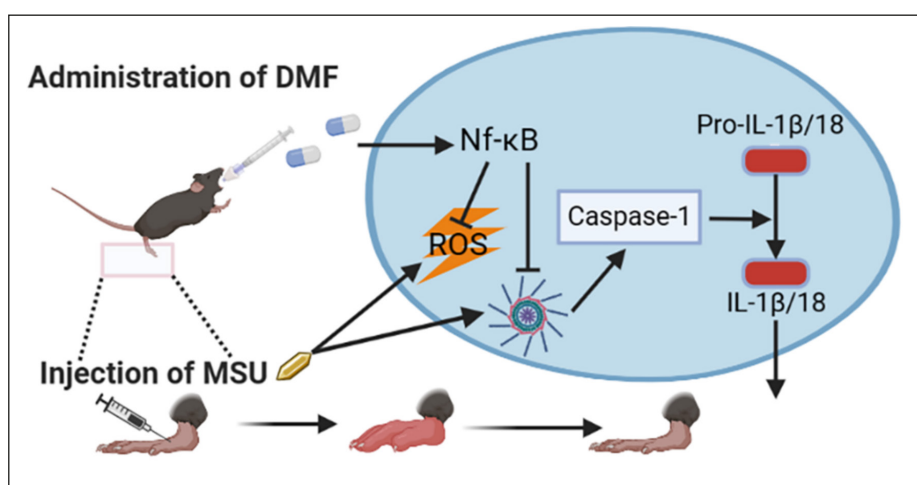


**Figure 5.** The underlying mechanism involved in the protective effects of DMF against gouty arthritis.

## Discussion

The incidence of gout is on the rise in recent years globally<sup>4,26</sup>. MSU crystal deposition is the clinicopathological basis of gouty arthritis, which seriously affects the life quality of patients<sup>27-29</sup>. The objective of this study was to investigate the therapeutic effects of DMF on MSU-induced inflammation and oxidative stress both *in vivo* and *in vitro*.

MSU crystal was injected into the ankle joint, the most common site in gouty patients, to establish the gouty arthritis mice model<sup>5</sup>. We found out that MSU-injected mice show significant gouty-related clinical manifestations, including joint swelling, mechanical hypersensitivity, and thermal sensitivity<sup>5,21,22</sup>. In this way, these clinical symptoms which can reflect the degree of improvement of acute joint, are widely used to assess the efficacy of anti-gouty treatment<sup>28,29</sup>. In our study, we first found that DMF possess the ability to restore the ankle swelling and hyperalgesia in MSU-induced acute gouty mice, and that higher doses of DMF are more effective. This apparent protective effect against gout symptoms motivates us to focus on the underlying mechanisms.

It is well known that inflammatory cytokines attack is involved in the acute gouty progress<sup>29,30</sup>. With the increase in uric acid levels in the blood, the urate crystal initially adhesion to the connective tissue near the joint, is supposed to fluctuate and falls off, diffusing into the joint cavity<sup>26,28</sup>. When MSU crystals are recognized and absorbed by macrophages, the inflammatory response control mechanism of the body is activated, thereby

worsening local inflammation, and increasing the recruitment of phagocytes to the joint<sup>3,30,31</sup>. Accumulating studies<sup>3,31</sup> have shown that multiple pro-inflammatory cytokines play critical roles in the pathogenesis of gouty arthritis. Released IL-1 $\beta$  from macrophages emerges to promote the expression of adhesion molecules and chemokines, together with other inflammatory events in endothelial cells, resulting in neutrophil recruitment and subsequently causes the initiation of gouty inflammation<sup>12,30</sup>. In addition, TNF- $\alpha$ , with the function of promoting fever and immunity moderation, can potentiate uric acid-induced IL-1 $\beta$  release<sup>32,33</sup>. Based on this, anti-IL-1 and TNF receptor treatments have been proven effective in relieving the symptoms of patients with gout<sup>5,33</sup>. Increasing evidence has also found that IL-33, which is thought to be important in rheumatoid arthritis, are widely involved in the inflammatory response of gout arthritis<sup>10,34,35</sup>. More importantly, these cytokines are not only the initiating factors but also the continuous inducing factors in uric acid induced inflammation<sup>30,36</sup>. Therefore, effective drug that inhibit the release of inflammatory factors in gouty inflammatory response are urgently needed.

DMF, as an anti-inflammatory, exerts its antioxidant effects and antiinflammation in several immune disordered disease<sup>16</sup>. In recent years, research has extended DMF to be employed in neuroprotection, heart disease and renal ischemia-reperfusion injury in mice<sup>17,18,37</sup>. Yan et al<sup>25</sup> found that DMF improves cognitive deficits in chronic cerebral hypoperfusion rats. Mouton et al<sup>37</sup> found that DMF preserves left ventricular in-

fart integrity following myocardial infarction. Clinical trials<sup>18,38</sup> also demonstrated that DMF intake could lead to a decline in brain lesions and decreased relapse rates in RRMS patients, which proved its safety and efficacy. Given the role of inflammation in the gouty, we determined to treat gout arthritis with DMF. According to the protocol of previous studies and our preliminary experiment<sup>9,17,21,39</sup>, we gavaged mice with two concentrations of DMF (10 mg/kg or 30 mg/kg, once daily, I.P) continuously for seven days, which has shown therapeutic effect in other disease models without any side effects. In addition to the significant relief in clinical symptoms, the therapeutic effect of DMF is supported by the apparent suppression of inflammatory cytokine levels in joint tissues. Elisa assay showed that DMF could significantly decrease the levels of proinflammatory cytokines, IL-1 $\beta$ , IL-6, TNF- $\alpha$  and IL-18, in the joint tissue of MSU crystal-induced mice. Meanwhile, the reduction of neutrophil recruitment mediated by DMF also ameliorated the pathological destruction of the joint. This evidence further deepens our understanding of the anti-inflammatory activities of DMF.

The NLRP3 inflammasome is responsible for the production of pro-inflammatory cytokine in gout, and NF- $\kappa$ B is a crucial transcription factor in the mediation of inflammasome activation<sup>40,41</sup>. Interestingly, DMF also inhibits the pro-inflammatory pathway NF- $\kappa$ B, thus downregulating the expression of NLRP3 and IL-1 $\beta$  and decreases inflammatory response. Analogously, it has previously been shown<sup>23</sup> that DMF suppresses NLRP3 inflammasome in the LPS-stimulated microglia and the dextran sulfate sodium induced experimental colitis model. The NLRP3 inflammasome is composed of the sensor molecule NLRP3, the adaptor protein ASC, and pro-caspase-1<sup>7,42</sup>. Previous study<sup>43,44</sup> reported that the expression of NLRP3 was upregulated in peripheral blood mononuclear cells and synovial cells from gout patients in the acute stage. Our data indicated that DMF could effectively inhibit the expression of NF- $\kappa$ B and NLRP3 in an MSU-induced inflammatory reaction *in vivo*. Subsequently, MSU was added to LPS-primed murine macrophages to promote NLRP3 activation to investigate the effect of DMF *in vitro*. The experimental data from MSU-treated Raw 264.7 cells suggested that DMF are capable of attenuating cell damage in a dose-dependent manner. Meanwhile, DMF gave rise to depressed NLRP3 inflammasome observed by fluorescence microscope after immunofluorescence staining

in MSU-treated Raw 264.7 cells, consistent with the results in animal experiments. Moreover, we found that DMF was active on inhibiting the activity of caspase-1 generated by MSU, limiting the pro-IL-1 $\beta$  cleaved to IL-1 $\beta$ , which further indicated the effect of DMF in suppression of MSU-induced inflammatory response *in vivo* and *in vitro*.

Oxidative stress is considered an important factor in the activation of NLRP3 inflammasome<sup>14,45</sup>. Previous literature has reported that MSU could enhance NLRP3 inflammasome activation by overproduction of ROS. The maturation of the IL-1 $\beta$  and caspase-1 depends on ROS, and in turn, excessive inflammatory factors will aggravate the explosion of ROS, thus forming a vicious cycle of inflammatory response and oxidative stress<sup>9,21,35</sup>. Under physiological conditions, intracellular ROS production and antioxidant defense are in a dynamic balance<sup>46</sup>. Oxidative stress may result in damage to critical cellular macromolecules, including DNA, lipids, and proteins<sup>46,47</sup>. The MDA level in hind paw tissue of mice was detected to reflect the degree of membrane peroxidation injury, and the results showed that DMF could significantly inhibit membrane peroxidation caused by MSU. Besides, DMF enhanced the activity of SOD, an important intracellular antioxidant enzyme, in the gouty arthritis mice. Similar results were observed in MSU-challenged Raw 264.7 cells detected by ROS-sensitive probe. Of course, given the close relationship between oxidative stress and mitochondrial function, more explorations on mitochondrial homeostasis should be the focus of our next work.

## Conclusions

Our study suggested that DMF plays an anti-inflammatory role in MSU-induced inflammation as shown in Figure 5 (created with BioRender.com). Mechanistically, we propose that DMF suppresses NLRP3 inflammasome activation and protects against oxidative stress, consequently reducing proinflammatory factors levels and alleviating the inflammatory response in gouty arthritis. We will further emphasize on the role of DMF after the occurrence of gout, which is in an urgent clinical need.

## Conflict of Interest

The Authors declare that they have no conflict of interests.

### Funding

None.

### Ethics Approval

The experimental procedures (Protocol#2021-B07) were approved by the Local Ethics and Animal Care Committee of the First People's Hospital of LouDi and performed in accordance with the National Institute of Health Guide for Care and Use of Laboratory Animals.

### Informed Consent

Not applicable.

### Availability of Data and Materials

Data supporting the findings of this study are available from the corresponding author upon reasonable request.

### Authors' Contributions

YC and J-M Z conceived and designed the study; YH and X-F J participated in the literature search and data collection; YC, YL, and YH reviewed and edited the manuscript. All authors read and approved the final manuscript.

### ORCID ID

Y. CAO: 0000-0003-4476-1728

Y. HU: 0000-0002-1378-7573

X.-F. JIN: 0000-0003-4231-2451

Y. LIU: 0000-0002-4922-3534

J.-M. ZOU: 0000-0002-8093-8765

## References

- Desai J, Steiger S, Anders HJ. Molecular Pathophysiology of Gout. *Trends Mol Med* 2017; 23: 756-768.
- Fitzgerald JD, Dalbeth N, Mikuls T, Brignardello-Petersen R, Guyatt G, Abeles AM, Gelber AC, Harrold LR, Khanna D, King C, Levy G, Libbey C, Mount D, Pillinger MH, Rosenthal A, Singh JA, Sims JE, Smith BJ, Wenger NS, Bae SS, Danve A, Khanna PP, Kim SC, Lenert A, Poon S, Qasim A, Sehra ST, Sharma TSK, Toprover M, Turgunbaev M, Zeng L, Zhang MA, Turner AS, Neogi T. 2020 American College of Rheumatology Guideline for the Management of Gout. *Arthritis Care Res (Hoboken)* 2020; 72: 744-760.
- Terkeltaub R. What makes gouty inflammation so variable? *BMC Med* 2017; 15: 158.
- Dehlin M, Jacobsson L, Roddy E. Global epidemiology of gout: prevalence, incidence, treatment patterns and risk factors. *Nat Rev Rheumatol* 2020; 16: 380-390.
- Lan Z, Chen L, Feng J, Xie Z, Liu Z, Wang F, Liu P, Yue X, Du L, Zhao Y, Yang P, Luo J, Zhu Z, Hu X, Cao L, Lu P, Sah R, Lavine K, Kim B, Hu H. Mechanosensitive TRPV4 is required for crystal-induced inflammation. *Ann Rheum Dis* 2021; 80: 1604-1614.
- Lin Y, Luo T, Weng A, Huang X, Yao Y, Fu Z, Li Y, Liu A, Li X, Chen D, Pan H. Gallic Acid Alleviates Gouty Arthritis by Inhibiting NLRP3 Inflammasome Activation and Pyroptosis Through Enhancing Nrf2 Signaling. *Front Immunol* 2020; 11: 580593.
- Mangan MSJ, Olhava EJ, Roush WR, Seidel HM, Glick GD, Latz E. Targeting the NLRP3 inflammasome in inflammatory diseases. *Nat Rev Drug Discov* 2018; 17: 588-606.
- Luo Y, Xiong B, Liu H, Chen Z, Huang H, Yu C, Yang J. Koumine Suppresses IL-1 $\beta$  Secretion and Attenuates Inflammation Associated With Blocking ROS/NF- $\kappa$ B/NLRP3 Axis in Macrophages. *Front Pharmacol* 2020; 11: 622074.
- Chen B, Li H, Ou G, Ren L, Yang X, Zeng M. Curcumin attenuates MSU crystal-induced inflammation by inhibiting the degradation of I $\kappa$ B $\alpha$  and blocking mitochondrial damage. *Arthritis Res Ther* 2019; 21: 193.
- Fattori V, Staurengo-Ferrari L, Zaninelli TH, Casagrande R, Oliveira RD, Louzada-Junior P, Cunha TM, Alves-Filho JC, Teixeira MM, Cunha FQ, Amaral FA, Verri WA, Jr. IL-33 enhances macrophage release of IL-1 $\beta$  and promotes pain and inflammation in gouty arthritis. *Inflamm Res* 2020; 69: 1271-1282.
- Yin C, Liu B, Wang P, Li X, Li Y, Zheng X, Tai Y, Wang C, Liu B. Eucalyptol alleviates inflammation and pain responses in a mouse model of gout arthritis. *Br J Pharmacol* 2020; 177: 2042-2057.
- Galvão I, Vago JP, Barroso LC, Tavares LP, Queiroz-Junior CM, Costa VV, Carneiro FS, Ferreira TP, Silva PM, Amaral FA, Sousa LP, Teixeira MM. Annexin A1 promotes timely resolution of inflammation in murine gout. *Eur J Immunol* 2017; 47: 585-596.
- Lin Q, Li S, Jiang N, Shao X, Zhang M, Jin H, Zhang Z, Shen J, Zhou Y, Zhou W, Gu L, Lu R, Ni Z. PINK1-parkin pathway of mitophagy protects against contrast-induced acute kidney injury via decreasing mitochondrial ROS and NLRP3 inflammasome activation. *Redox Biol* 2019; 26: 101254.
- Abderrazak A, Syrovets T, Couchie D, El Hadri K, Friguet B, Simmet T, Rouis M. NLRP3 inflammasome: from a danger signal sensor to a regulatory node of oxidative stress and inflammatory diseases. *Redox Biol* 2015; 4: 296-307.
- Blair HA. Dimethyl Fumarate: A Review in Relapsing-Remitting MS. *Drugs* 2019; 79: 1965-1976.
- Saidu NEB, Kavian N, Leroy K, Jacob C, Nicco C, Batteux F, Alexandre J. Dimethyl fumarate, a two-edged drug: Current status and future directions. *Med Res Rev* 2019; 39: 1923-1952.



- 17) Yang Y, Cai F, Zhou N, Liu S, Wang P, Zhang S, Zhang Y, Zhang A, Jia Z, Huang S. Dimethyl fumarate prevents ferroptosis to attenuate acute kidney injury by acting on NRF2. *Clin Transl Med* 2021; 11: e382.
- 18) Liebmann M, Korn L, Janoschka C, Albrecht S, Lauks S, Herrmann AM, Schulte-Mecklenbeck A, Schwab N, Schneider-Hohendorf T, Eveslage M, Wildemann B, Luessi F, Schmidt S, Diebold M, Bittner S, Gross CC, Kovac S, Zipp F, Derfuss T, Kuhlmann T, König S, Meuth SG, Wiendl H, Klotz L. Dimethyl fumarate treatment restrains the antioxidative capacity of T cells to control autoimmunity. *Brain* 2021; 144: 3126-3141.
- 19) Sulaimani J, Cluxton D, Clowry J, Petrasca A, Molloy OE, Moran B, Sweeney CM, Malara A, McNicholas N, Mcguigan C, Kirby B, Fletcher JM. Dimethyl fumarate modulates the Treg-Th17 cell axis in patients with psoriasis. *Br J Dermatol* 2021; 184: 495-503.
- 20) Takasu C, Vaziri ND, Li S, Robles L, Vo K, Takasu M, Pham C, Farzaneh SH, Shimada M, Stamos MJ, Ichii H. Treatment with dimethyl fumarate ameliorates liver ischemia/reperfusion injury. *World J Gastroenterol* 2017; 23: 4508-4516.
- 21) Wang Y, Zhu W, Lu D, Zhang C, Wang Y. Tetrahydropalmitine attenuates MSU crystal-induced gouty arthritis by inhibiting ROS-mediated NLRP3 inflammasome activation. *Int Immunopharmacol* 2021; 100: 108107.
- 22) Martinov T, Mack M, Sykes A, Chatterjea D. Measuring changes in tactile sensitivity in the hind paw of mice using an electronic von Frey apparatus. *J Vis Exp* 2013; e51212.
- 23) Reda HM, Zaitone SA, Moustafa YM. Effect of levetiracetam versus gabapentin on peripheral neuropathy and sciatic degeneration in streptozotocin-diabetic mice: Influence on spinal microglia and astrocytes. *Eur J Pharmacol* 2016; 771: 162-172.
- 24) Tastan B, Arioiz BI, Tufekci KU, Tarakcioglu E, Gonul CP, Genc K, Genc S. Dimethyl Fumarate Alleviates NLRP3 Inflammasome Activation in Microglia and Sickness Behavior in LPS-Challenged Mice. *Front Immunol* 2021; 12: 737065.
- 25) Yan N, Xu Z, Qu C, Zhang J. Dimethyl fumarate improves cognitive deficits in chronic cerebral hypoperfusion rats by alleviating inflammation, oxidative stress, and ferroptosis via NRF2/ARE/NF- $\kappa$ B signal pathway. *Int Immunopharmacol* 2021; 98: 107844.
- 26) Dalbeth N, Merriman TR, Stamp LK. Gout. *Lancet* 2016; 388: 2039-2052.
- 27) Dalbeth N, Choi HK, Joosten LaB, Khanna PP, Matsuo H, Perez-Ruiz F, Stamp LK. Gout. *Nat Rev Dis Primers* 2019; 5: 69.
- 28) Stamp LK, Dalbeth N. Prevention and treatment of gout. *Nat Rev Rheumatol* 2019; 15: 68-70.
- 29) Yip K, Berman J. What Is Gout? *Jama* 2021; 326: 2541.
- 30) So AK, Martinon F. Inflammation in gout: mechanisms and therapeutic targets. *Nat Rev Rheumatol* 2017; 13: 639-647.
- 31) Schauer C, Janko C, Munoz LE, Zhao Y, Kienhöfer D, Frey B, Lell M, Manger B, Rech J, Naschberger E, Holmdahl R, Krenn V, Harrer T, Jeremic I, Bilyy R, Schett G, Hoffmann M, Herrmann M. Aggregated neutrophil extracellular traps limit inflammation by degrading cytokines and chemokines. *Nat Med* 2014; 20: 511-517.
- 32) Saha P, Smith A. TNF- $\alpha$  (Tumor Necrosis Factor- $\alpha$ ). *Arterioscler Thromb Vasc Biol* 2018; 38: 2542-2543.
- 33) Yokose K, Sato S, Asano T, Yashiro M, Kobayashi H, Watanabe H, Suzuki E, Sato C, Kozuru H, Yatsuhashi H, Migita K. TNF- $\alpha$  potentiates uric acid-induced interleukin-1 $\beta$  (IL-1 $\beta$ ) secretion in human neutrophils. *Mod Rheumatol* 2018; 28: 513-517.
- 34) Yin C, Liu B, Li Y, Li X, Wang J, Chen R, Tai Y, Shou Q, Wang P, Shao X, Liang Y, Zhou H, Mi W, Fang J, Liu B. IL-33/ST2 induces neutrophil-dependent reactive oxygen species production and mediates gout pain. *Theranostics* 2020; 10: 12189-12203.
- 35) Renaudin F, Orliaguet L, Castelli F, Fenaille F, Prignon A, Alzaid F, Combes C, Delvaux A, Adimy Y, Cohen-Solal M, Richette P, Bardin T, Riveline JP, Venteclef N, Lioté F, Campillo-Gimenez L, Ea HK. Gout and pseudo-gout-related crystals promote GLUT1-mediated glycolysis that governs NLRP3 and interleukin-1 $\beta$  activation on macrophages. *Ann Rheum Dis* 2020; 79: 1506-1514.
- 36) Cabău G, Crişan TO, Klück V, Popp RA, Joosten LaB. Urate-induced immune programming: Consequences for gouty arthritis and hyperuricemia. *Immunol Rev* 2020; 294: 92-105.
- 37) Mouton AJ, Flynn ER, Moak SP, Aitken NM, Omoto ACM, Li X, Da Silva AA, Wang Z, Do Carmo JM, Hall JE. Dimethyl fumarate preserves left ventricular infarct integrity following myocardial infarction via modulation of cardiac macrophage and fibroblast oxidative metabolism. *J Mol Cell Cardiol* 2021; 158: 38-48.
- 38) Vucic S, Henderson RD, Mathers S, Needham M, Schultz D, Kiernan MC. Safety and efficacy of dimethyl fumarate in ALS: randomised controlled study. *Ann Clin Transl Neurol* 2021; 8: 1991-1999.
- 39) Ashrafian H, Czibik G, Bellahcene M, Aksentijevic D, Smith AC, Mitchell SJ, Dodd MS, Kirwan J, Byrne JJ, Ludwig C, Isackson H, Yavari A, Stottrup NB, Contractor H, Cahill TJ, Sahgal N, Ball DR, Birkler RI, Hargreaves I, Tennant DA, Land J, Lygate CA, Johannsen M, Kharbanda RK, Neubauer S, Redwood C, De Cabo R, Ahmet I, Talan M, Gunther UL, Robinson AJ, Viant MR, Pollard PJ, Tyler DJ, Watkins H. Fumarate is cardioprotective via activation of the Nrf2 antioxidant pathway. *Cell Metab* 2012; 15: 361-371.
- 40) Afonina IS, Zhong Z, Karin M, Beyaert R. Limiting inflammation—the negative regulation of NF- $\kappa$ B and the NLRP3 inflammasome. *Nat Immunol* 2017; 18: 861-869.
- 41) Sun SC. The non-canonical NF- $\kappa$ B pathway in immunity and inflammation. *Nat Rev Immunol* 2017; 17: 545-558.

- 42) He Y, Hara H, Núñez G. Mechanism and Regulation of NLRP3 Inflammasome Activation. *Trends Biochem Sci* 2016; 41: 1012-1021.
- 43) Dalbeth N, Gosling AL, Gaffo A, Abhishek A. Gout. *Lancet* 2021; 397: 1843-1855.
- 44) Goldberg EL, Asher JL, Molony RD, Shaw AC, Zeiss CJ, Wang C, Morozova-Roche LA, Herzog RI, Iwasaki A, Dixit VD.  $\beta$ -Hydroxybutyrate Deactivates Neutrophil NLRP3 Inflammasome to Relieve Gout Flares. *Cell Rep* 2017; 18: 2077-2087.
- 45) Ferrucci L, Fabbri E. Inflammageing: chronic inflammation in ageing, cardiovascular disease, and frailty. *Nat Rev Cardiol* 2018; 15: 505-522.
- 46) Forman HJ, Zhang H. Targeting oxidative stress in disease: promise and limitations of antioxidant therapy. *Nat Rev Drug Discov* 2021; 20: 689-709.
- 47) Szczepanik FSC, Grossi ML, Casati M, Goldberg M, Glogauer M, Fine N, Tenenbaum HC. Periodontitis is an inflammatory disease of oxidative stress: We should treat it that way. *Periodontol* 2000 2020; 84: 45-68.